

Diagnostic plots applied to well-tests in karst systems

Jean-Christophe Maréchal, Bernard Ladouche, Benoît Dewandel, Perrine Fleury, Nathalie Dörfliger
BRGM, D3E/NRE, 1039 rue de Pinville, F-34000 Montpellier, jc.marechal@brgm.fr

Abstract

Pumping tests conducted on wells intersecting karst heterogeneities such as the conduit network are difficult to interpret. Nevertheless, this case can be solved by assimilating the horizontal karst conduit to a finite-conductivity vertical fracture. In this case, several flow patterns corresponding to the respective contributions of karst subsystems (fractured matrix, small conduits and main karst drainage network) can be identified on the diagnostic plot of drawdown derivative.

This is illustrated on two examples from Mediterranean karst systems. A pumping test on a well crossing the main karst drainage network of the Cent-Fonts karst system shows (i) a preliminary contribution of the karst conduit storage capacity followed by (ii) linear flows into the fractured matrix. A pumping test on a well intersecting a small karst conduit of the Bas-Agely karst system shows the existence of (i) bi-linear flows within both the karst conduit and the fractured matrix at early times, followed by (ii) radial flows within the fractured matrix and (iii) finally the contribution of a major karst cavity.

The use of diagnostic plots allows identifying the various flow regimes during pumping tests, corresponding to the response of the individual karst aquifer subsystems. This is helpful in order to understand the structure of the karst aquifer and flow exchanges between subsystems.

1. Introduction

Due to the complexity and duality of flows, well-test interpretation into karst systems constitutes a challenging task for hydrogeologists (KRESIC 2007). This is especially true when the pumping well intersects karst heterogeneities such as the conduit network for example. Nevertheless, well-tests can bring valuable information on the presence and size of karst heterogeneities.

Diagnostic plots of drawdown derivative have been widely used in oil industry for fractured reservoirs characterization. These techniques are now used by hydrogeologists (MARÉCHAL et al. 2004; RENARD et al. 2009) in order to establish conceptual models of fractured aquifers under pumping. This method can be applied to karst hydrogeology as well. In this paper, the classical response of a well-test into a large fracture (or karst conduit) is described on a log-log drawdown derivative curve. It allows identifying successive flow regimes corresponding to the contribution of various karst aquifer subsystems (fractured matrix within the vadose zone, karst conduit, main karst drainage network) to the pumped well. The interpretation of such a diagnostic plot is illustrated on two examples from Mediterranean karst systems.

2. Method

In heterogeneous karst systems, the log-log diagnostic plot of drawdown and its derivative in the pumping well or in observation wells can help identifying departures in flow-geometry from the classical homogeneous radial case. The common logarithm of drawdown s change is plotted versus the logarithm of elapsed time t , together with $\log(ds/d \ln t)$, the logarithm of the derivative of drawdown change with respect to the natural logarithm of time. Several authors (EHLIG-ECONOMIDES 1988) noticed that the drawdown derivative displays late-time straight lines, with slopes related to the domain dimensionality and boundary conditions. Classically, the log-log diagnostic plot can be divided into several portions with: (a) early data used for identifying the wellbore or karst conduit storage; (b) intermediate data for identifying the type of aquifer model that should be used (e.g. double porosity, unconfined, drainage); and (c) late data for identifying the possible boundaries.

Sitting a pumping well on the karst conduit network (Fig. 1) of a karst system constitutes an interesting target regarding further possible karst aquifer exploitation. This position of the pumping well allows draining the highly permeable karst conduit which will then interact with the surrounding matrix. The karst conduit constitutes then a useful extension of the pumping well. Two separate cases are distinguished: (a) the case of a pumping well intersecting the main karst drainage network connected to the outlet (PWa in Fig. 1) and (b) the case of a pumping well intersecting a small karst conduit (PWB in Fig. 1).

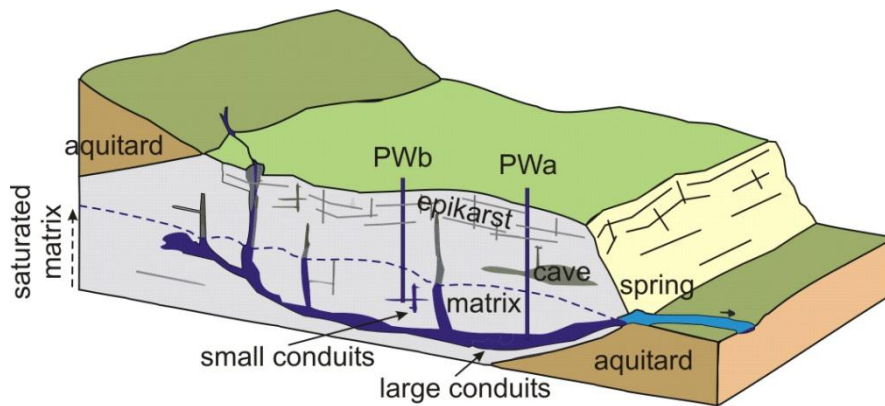


Fig. 1: Karst aquifer with a pumping-well (PW) located into the karst conduit network (modified from GOLSCHEIDER & DREW 2007): PWa pumping well crossing the main karst drainage network; PWb pumping well crossing a small karst conduit

These cases can be compared to wells stimulated by hydraulic fracturing techniques as described in the petroleum literature. Consider a vertically fractured well producing at a constant flow rate in an infinite, isotropic, homogeneous horizontal aquifer. Fig. 2 shows the general behaviour of a well with a horizontal conduit that can be assimilated to a finite-conductivity vertical fracture. The flow-pattern geometry under such conditions will change with time and includes several flow periods (CINCO-LEY & SAMANIEGO-V 1981). During early pumping times (Fig. 2a), conduit linear flow (conduit or wellbore storage effect) is characterized by a straight line with a slope $\nu = 1$ on the diagnostic plot. After a transition flow period, the system may or may not exhibit a bi-linear flow period (Fig. 2b), indicated by a one-fourth-slope straight line that lasts as long as the conduit boundaries do not affect the flow pattern. As time increases, the flow in the matrix becomes one-dimensional (horizontal, parallel and perpendicular to the conduit) as illustrated on Figure 2c. On a diagnostic plot, the slope of the derivative curve is $\nu = 0.5$. As pumping continues, the flow pattern can change from parallel flow to pseudo-radial flow (Fig. 2d). During this period, the pumped water originates from farther away and the local effect of the finite-length conduit tends to disappear. The drawdown curve tends to the Jacob straight line with a slope $\nu = 0$ of the derivative at late times, but this would arise only if the duration of the pumping test is very long. This four-period flow-pattern geometry makes it impossible to interpret such drawdown curves with classical techniques. The corresponding typical drawdown and derivative curves (diagnostic plot) are illustrated on Fig. 2e.

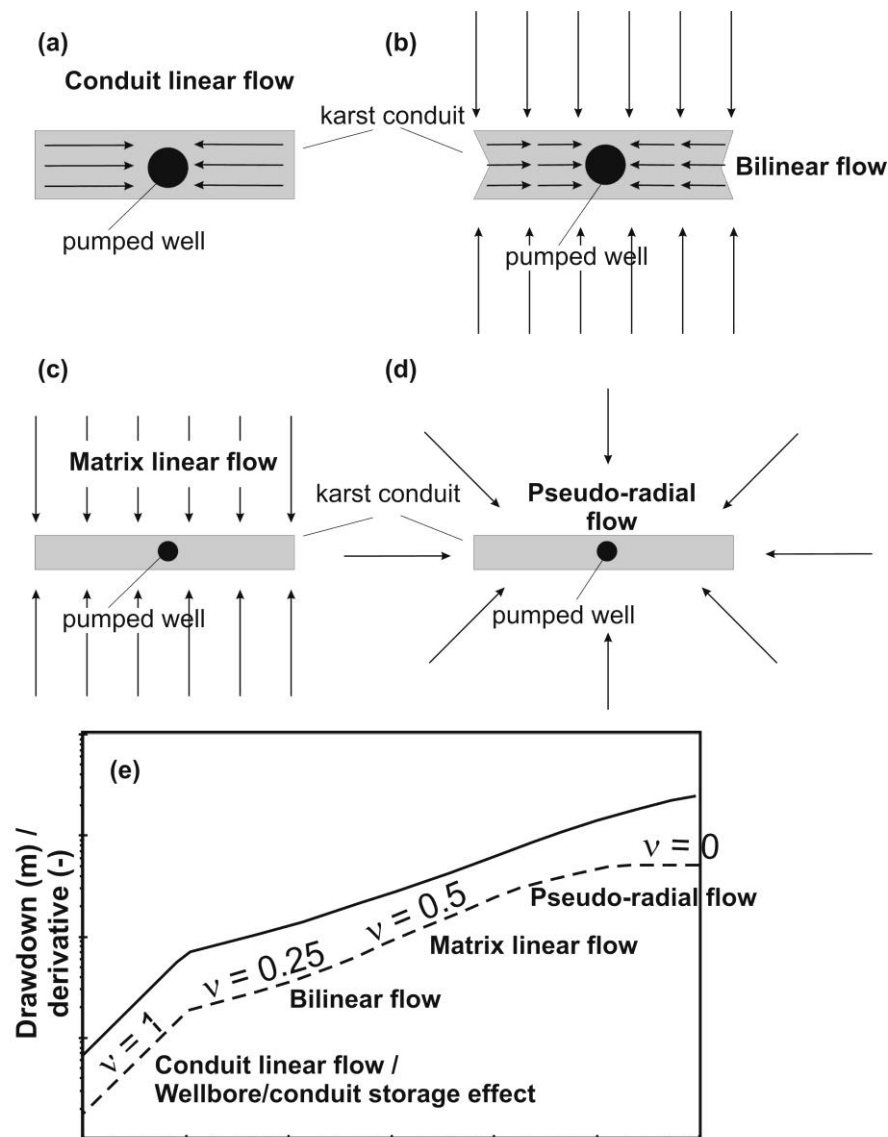


Fig. 2: A well intersecting a karst conduit acting as a vertical fracture of finite length and finite hydraulic conductivity: (a) Linear flow in the conduit or wellbore/conduit storage effect during early pumping times; (b) Bi-linear flow; (c) Matrix linear flow; (d) Matrix pseudo-radial flow during late pumping times, modified after (CINCO-LEY & SAMANIEGO-V, 1981); (e) Diagnostic plot of the same case

3. Study areas

The Cent-Fonts karst (Fig.3) is a mixed-flow karst system located north of Montpellier (Hérault region, Southern France) in a thick limestone and dolomite series (Middle and Upper Jurassic). It has been characterized by long-term monitoring (1997-2007) and numerous studies [Ladouche et al., 1999, 2002, 2005, 2006a; Aquilina et al., 1999, 2005, 2006]. The Cent-Fonts spring, located on the right bank of the Hérault River, is the only outlet of the karst system (Fig.3a). Its discharge ranges from $Q_S = 220$ L/s (during severe low water stage periods) to more than 12,000 L/s during peak flow in winter or spring, the average spring discharge having been about 1 m³/s during the 1997-2005 period [Ladouche et al, 2005]. The Cent-Fonts spring is the outlet of a water-saturated karst conduit network that has been partially explored and mapped by divers in the vicinity of the spring, particularly for the purpose of the pumping well sitting [Bardot, 2001 in Ladouche et al., 2005]. The network is developed below the Hérault River to a depth of at least

95 m (Fig. 3b). In the mapped area, the cross-sectional area of the karst drain ranges from 4 m^2 to 16 m^2 and its largest part (a 400 m^3 cavity) is located at the end of the explored karst conduit (Fig. 3b). Three wells intercept the karst network near the spring (Fig. 3b): CGE is about 60 m deep, F3 is located about 100 meters upstream from CGE and reaches the largest part of the conduit at a depth of 128 m, and F2 is located 3 meters from F3 in the same conduit.

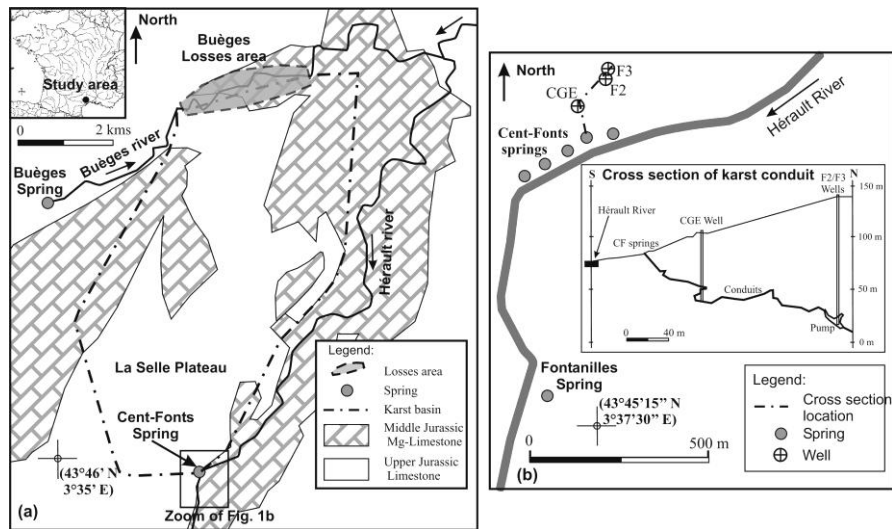


Fig. 3: (a) Geological and location map of the Cent-Fonts karst system. (b) Location of pumping well (F3); cross section showing the wells intersecting the conduit network

The Bas-Agly karst system is located on the Mediterranean coast in Southern France (Pyrénées-Orientales), near the Salses-Leucate lagoon (DORFLIGER & al. 2009). Due to the complex tectonics of the Corbières, strongly influenced by Pyrenean orogenesis, the Jurassic-Cretaceous limestone aquifer is not a continuous aquifer. The depth of karstification, several hundreds of meters below sea level, is linked to the Messinian Salinity Crisis. This system is partially cut off from the Mediterranean Sea by the Plio-Quaternary sedimentary cover. To the North, the karst is in contact with the brackish Salses-Leucate lagoon (Fig. 4). The two main springs of this karst system are the Font Estramar spring and the Font Dame spring, which merge near the brackish lagoon, a few kilometers from each other. The Font Dame spring is characterized by several outlets in a wetland with a low water stage discharge of 300 L/s and a high water stage discharge of 6000 L/s. The Font Estramar spring is located at the foot of a Cretaceous limestone cliff. Its discharge is between 800 L/s and more than 20,000 L/s. The total mean annual flow rate for the two springs is 2500 L/s (1700 L/s at Font Estramar and 800 L/s at Font Dame).

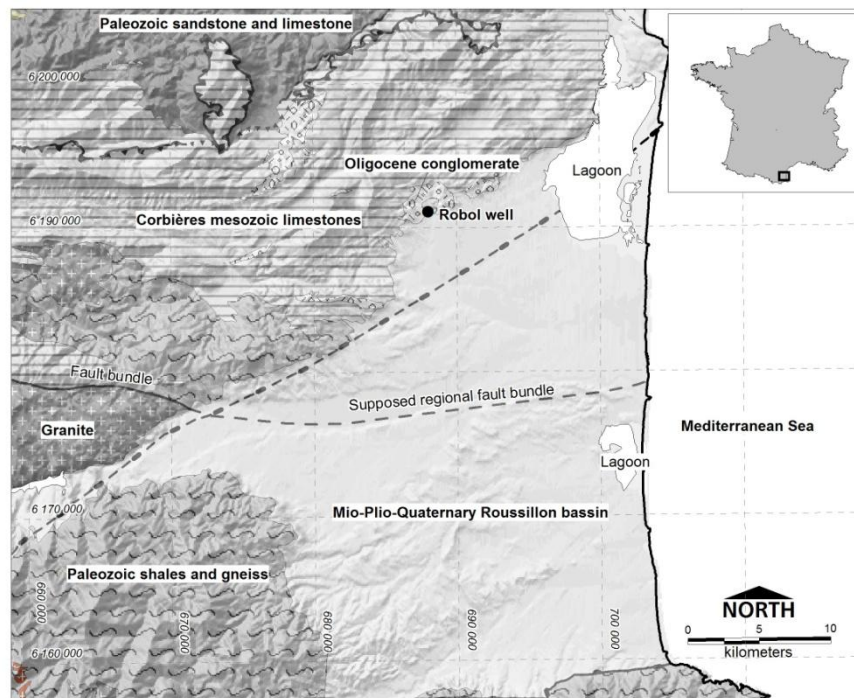


Fig. 4: (a) Geological and location map of the Bas-Agly karst system and Robol well

4. Results

4.1. Cent-Fonts karst system

A long-duration pumping test (one month) was conducted on the main conduit of the Cent-Fonts karst system (MARECHAL et al. 2008). The well F3 has been sited by diving exploration in order to intersect the main karst conduit about 100 m upstream from the spring of the system (Fig. 1b). The well was pumped at a constant discharge rate of 400 L/s. During the first 24 hours (≈ 1500 minutes), the storage effect in the karst conduit prevailed (slope $\nu = 1$, Fig. 5a). After that, the drawdown tended to linear flow with a slope decreasing to $\nu = 0.7$. No bi-linear flow period was observed. In fractured systems, CINCO-LEY & SAMANIEGO-V (1981) consider that this behaviour is not present when the fracture has a high storage capacity and a high conductivity. This is the most probable reason for such behaviour, given the large diameter (3.5 m) of the karst conduit in the vicinity of the pumping well.

Analytical solutions for a pumping well intersecting a vertical fracture of infinite conductivity can be transposed to a well intersecting a high-conductivity karst conduit. Such solutions were developed by petroleum engineers for application to artificially fractured wells (KRUSEMAN & RIDDER 1990). They deal with a fully penetrating, vertically fractured well pumped at a constant rate, in an ideal, homogeneous, and horizontal formation (corresponding to the matrix in the karst system) of constant thickness, porosity (S_m) and permeability (T_m).

In case the storage capacity of the pumped well and conduit is low, the fracture is idealized as a planar surface of zero thickness and infinite hydraulic conductivity, such that there is no hydraulic-head drop as water flows internally through the fracture to the well (GRINGARTEN & RAMEY 1974a). In addition, if the well or the pumped conduit are large enough to induce a significant well-storage effect, a modified solution can be applied (GRINGARTEN & RAMEY 1974b; RAMEY & GRINGARTEN 1976). This storage volume involves all high-hydraulic conductivity volumes that communicate with the well. It is represented by C_{vf} , defined as the ratio between the change in volume of water in the well plus karst conduit, and the corresponding drawdown. This parameter corresponds to the free-surface area of the dewatering conduit network (vertical shafts and variably saturated conduits). Although cited in hydrogeological literature, field examples of these analytical solutions are rare (KRUSEMAN & RIDDER 1990).

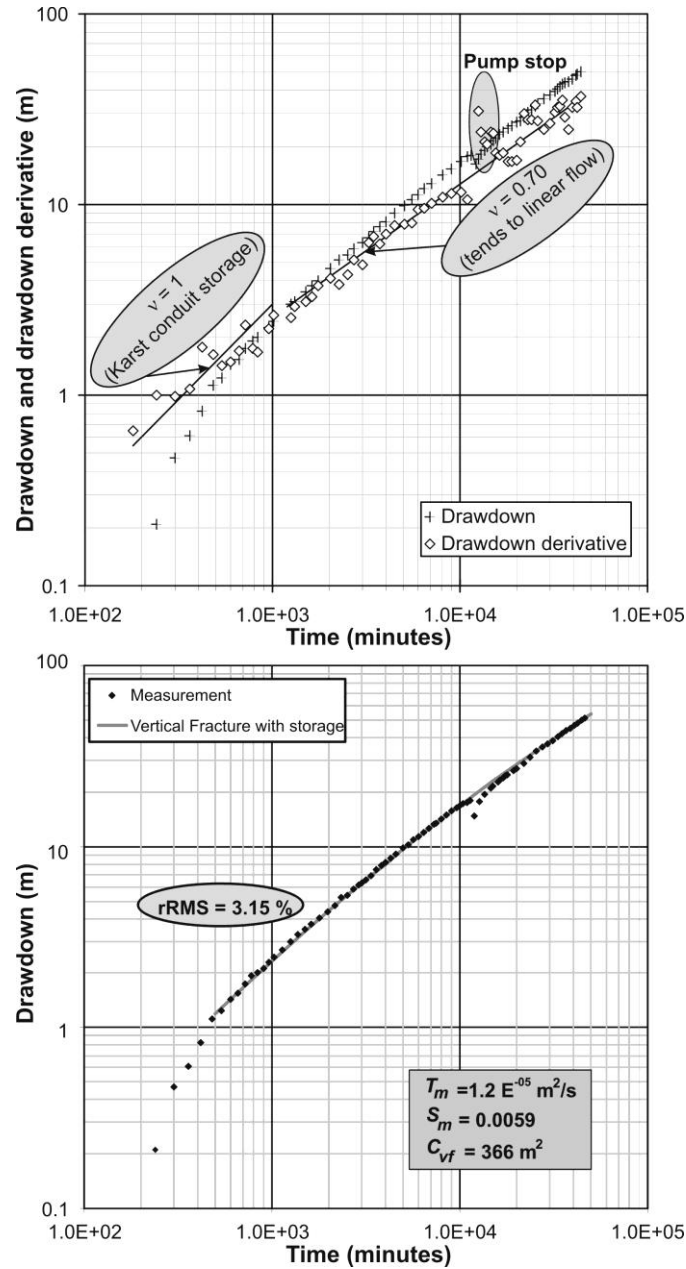


Fig. 5: (a) Diagnostic plot of the Cent-Fonts pumping test; (b) Temporal evolution of measured drawdown and fitting with the single-vertical-fracture method of (RAMEY & GRINGARTEN, 1976), modified after (MARÉCHAL et al., 2008)

The fit of the vertical fracture with the storage model on measured data is quite good after 10 hours (rRMS = 3.15%, Figure 5b). Using the hypothesis of a 5000-m-long karst conduit, the obtained hydrodynamic parameters are given on Figure 5b. During this test, no pseudo-radial flow period was observed. This is most probably due to the great length of the karst network.

4.2. Bas-Aglykarst system

The Robol well was drilled in the Bas-Agly karst system near Perpignan (Fig. 4). With a total depth of 500 m, a karst conduit with an approximate diameter of 10 cm was intersected at 420 m depth. The diagnostic plot of the long-duration pumping test shows three phases (Fig. 6):

- During the first 20 minutes, the flow regime was characterized by a slope $\nu = 0.2 - 0.3$ corresponding to bi-linear flow (linear flow in the conduit and in the fractured matrix);

- Between 20 and 100 minutes, the drawdown derivative was constant ($v = 0$) corresponding to a pseudo-radial flow regime within the matrix. The transmissivity of the matrix was determined to be $2.5 \cdot 10^{-4} \text{ m}^2/\text{s}$;
- After 100 minutes, the derivative strongly decreased because of stabilized drawdown due to a constant head boundary condition most probably corresponding to another large karst volume.

No conduit linear-flow regime was observed at the beginning of the test because the radius of the intersected karst conduit is small and its storage effect is therefore not measurable. The early transition to a pseudo-radial flow regime is due to the limited length of the karst conduit compared, for example, to the Cent-Fonts karst conduit. Therefore, no linear flow within the fractured matrix is observed.

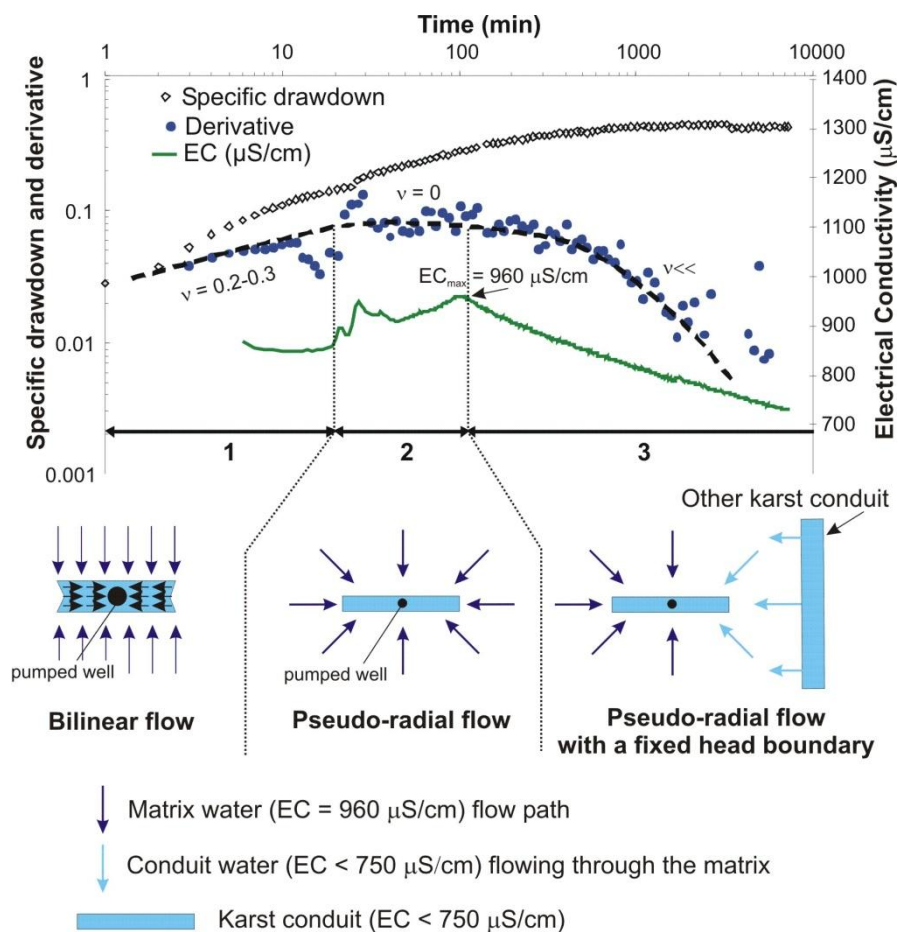


Fig. 6: Pumping test in the Robol well, intersecting a deep small karst conduit

These changes in flow regimes induce fluctuations in the electrical conductivity (EC) of the pumped water (Fig.6). Let us assume that the pumped water results from the mixing of two end-members: less mineralized (low EC) conduit water and more mineralized (high EC) matrix water. During the first phase, the EC is medium because the water is a mix of conduit and matrix water. During the second phase, the EC increases as the matrix contribution increases: the maximum value reaches $EC_{\text{max}} = 960 \mu\text{S}/\text{cm}$. Once the effect of another karst conduit is observed on the drawdown derivative (Phase 3), the water EC decreases toward that of the karst conduit water ($\leq 750 \mu\text{S}/\text{cm}$). The rapid EC decrease suggests the existence of a direct relationship between two karst volumes. This could be either a fracture network between two separate karst conduits, or a constriction separating a single karst conduit in two parts. Interestingly, the sharp EC increase of the water after 20-25 minutes induced by increased pumping rates was due to matrix-water inflow; the small pumped karst conduit could not provide the necessary water, which consequently flowed in from the matrix.

5. Conclusion

Classical methods for pumping tests interpretation cannot be applied to wells intersecting karst heterogeneities. Nevertheless, the use of diagnostic plots allows identifying various flow regimes during pumping tests, corresponding to the response of the individual karst aquifer subsystems (fractured matrix, small conduits, and main karst drainage network). The succession of various flow regimes brings information about the complexity of flow processes within the karst system. This is helpful in order to understand the structure of the karst aquifer and flow exchanges between subsystems.

Acknowledgements

This research project was funded by BRGM as part of the Corbières Phase 3 and EAUR15-R2EAU projects. The General Councils of Aude and of Pyrénées-Orientales, the Regional Council of Languedoc-Roussillon and Rhône, and the Mediterranean and Corsica Water Agency (AERM&C) also provided financial support.

References

- Cinco-Ley H. & Samaniego-V F. 1981. *Transient pressure analysis for fractured wells. Journal of Petroleum Technology*, 33(9): 1749-1766.
- Dörfliger N., Fleury P. & Ladouche B. 2009. *Inverse Modeling Approach to Allogenic Karst System Characterization. Ground Water* 47(3), 414-426.
- Ehlig-Economides C. 1988. *Use of the pressure derivative for diagnosing pressure-transient behavior. Journal of Petroleum Technology*: 1280-1282.
- Goldscheider N. & Drew D.P. 2007. *Methods in Karst hydrogeology. Taylor & Francis Group.*
- Gringarten A.C. & Ramey H.J. 1974a. *Unsteady-state pressure distribution created by a well with a single horizontal fracture, partially penetrating or restricted entry. Trans. Am. Inst. Min. Eng.*, 257: 413-426.
- Gringarten A.C. & Ramey H.J. 1974b. *Unsteady-state pressure distributions created by a well with a single infinite-conductivity vertical fracture. Society of Petroleum Engineers Journal*, August: 347-360.
- Kresic N. 2007. *Hydraulic methods, in: Methods in karst hydrogeology / edited by Nico Goldscheider & David Drew. Taylor & Francis Group.*
- Kruseman G.P. & Ridder N.A. 1990. *Analysis and evaluation of pumping test data. ILRI Publication.*, 377 pp.
- Maréchal J.C., Dewandel B. & Subrahmanyam K. 2004. *Use of hydraulic tests at different scales to characterize fracture network properties in the weathered-fractured layer of a hard rock aquifer. Water Resources Research*, 40(11).
- Maréchal J.C., Ladouche B., Dorfliger N. & Lachassagne P., 2008. *Interpretation of pumping tests in a mixed flow karst system. Water Resources Research*, 44(5).
- Ramey H.J. & Gringarten A.C. 1976. *Effect of high-volume vertical fractures on geothermal steam well behavior. U.S. Government Printing Office*, pp. 1759-1762.
- Renard P., Glenz D. & Mejias M. 2009. *Understanding diagnostic plots for well-test interpretation. Hydrogeology Journal*, 17(3): 589-600.